QR code as speckle pattern for reinforced concrete beams using digital image correlation

B. Murali Krishna[*], T.P. Tezeswi, P. Rathish Kumar, K. Gopikrishna,
M.V.N. Sivakumar and M. Shashi

Department of Civil Engineering, National Institute of Technology Warangal, Telangana, India-506004

Abstract. Digital Image Correlation technique (DIC) is a non-contact optical method for rapid structural health monitoring of critical infrastructure. An innovative approach to DIC is presented using QR (Quick Response) code based random speckle pattern. Reinforced Cement Concrete (RCC) beams of size 1800 mm x150 mm x 200 mm are tested in flexure. DIC is used to extract Moment (M) – Curvature (κ) relationships using random speckle patterns and QR code based random speckle patterns. The QR code based random speckle pattern is evaluated for 2D DIC measurements and the QR code speckle pattern performs satisfactorily in comparison with random speckle pattern when considered in the context of serving a dual purpose. Characteristics of QR code based random speckle pattern are quantified and its applicability to DIC is explored. The ultimate moment-curvature values computed from the QR code based random speckled pattern are found to be in good agreement with conventional measurements. QR code encrypts the structural information which enables integration with building information modelling (BIM).

Keywords: DIC; Speckle Pattern; QR Code; Moment-Curvature; Reinforced Cement Concrete (RCC)

1. Introduction

Indian Railways has more than 0.13 million bridges, out of which 800 are important, 11,000 are major and 0.12 million are minor bridges. There are 5174 large dams (maximum height of more than 15 m) in India with more than half of these aged at least 30 years. The cost of monitoring each and every one of these structures is astronomical. DIC is an established, simple cost-effective and practical imaging-based technique for condition monitoring of bridges, dams, nuclear industry, defense and aerospace structures. DIC enables determination of the surface deformation of an object (Mudassar and Butt 2016). The deformation components on the surface of an object are obtained using DIC algorithms by recording the images of the surface before as well as after loading. The algorithms available in the literature are Curve Fitting Gradient-Based, and Newton-Raphson Algorithms. Among these algorithms, Newton-Raphson Algorithm gives stable results with more accuracy (Lu and Cary 2000, Vassoler and Fancello 2010, Cofaru *et al.* 2010, Yuan *et al.* 2015). However in some of the algorithms Su and Anand (2003) accuracy and speed are not verified, while algorithms developed by Kozicki and Tejchman (2007) is highly expensive.

∗Corresponding author, Research Scholar, E-mail: bmurali@student.nitw.ac.in

Several researchers have applied the Gradient-Based Algorithm to DIC (Long *et al.* 2013).

Portable DIC and non-interferometric methods are widely used in the field of structural health monitoring (Antos *et al.* 2017). The non-interferometric method determines the surface distortion by evaluating the gray intensity variations of the object surface before as well as after deformation, and normally have less rigorous expectations under experimental conditions (Pan *et al.* 2009). DIC technique has been extensively accepted and frequently used as an effective and versatile tool for surface distortion measurement as part of experimental solid mechanics. This method is based on correlating the digital images associated with an object before and after deformation and, additionally identifying the displacement and strain field for an object, depending upon the position of the image (Sutton *et al.* 2009).

In the present study rectangular concrete beam specimens are tested under flexure in a UTM (Universal testing machine). Strains and deformations are computed using both random speckle and QR code based random speckle patterns applied on the specimens. Matlab® based open source DIC software package Ncorr V1.2.2 is employed for image processing. Ncorr is an open-source subset based 2D (Two Dimensional) DIC software that includes modern DIC algorithms with some additional enhancements (Blaber *et al.* 2015). Ncorr software was used to compare results of contact sensor devices, connected to the specimen with those obtained by dial gauges.

An important aspect of DIC is to provide an appropriate pattern on the sample to be tested, which has significant impact on the quality of results; hence it is important to achieve an optimal pattern initially. All patterns irrespective of length scales should be spatially random. The randomness assures that the DIC monitoring algorithm works properly. Systematic studies were performed by previous researchers to determine the quality of contrasting speckle patterns on the surface of test specimens that have a dominant influence on the spatial resolution and accuracy of results (Carter *et al.* 2015, Bossuyt 2013). It is concluded that to achieve an effective correlation, the pattern must be random, isotropic and highly contrasting. In addition to this, speckles should be neither too small nor too large. Consistent speckle sizes has to be maintained ideally 3-5 pixels in size. Correlation may fail with extremely large or small speckle pattern. The size of the speckles combined with the size of the used pixel subset influences the accuracy of the measured displacements (Salmanpour and Mojsilovic 2013, Lecompte *et al.* 2006). If the pattern is too large, certain subsets may be entirely on a black field or entirely on a white field. Conversely, very minute speckles can cause aliasing effect resulting in images that often show a pronounced moire pattern in the measurement result. Strain resolution increases with increase in speckle density from 23% to 58% of area fraction. Speckle patterns containing medium-sized speckles and exhibiting a limited spectral content yield the most accurate displacement measurements. Patterns well-suited for DIC exhibit a sharp correlation peak, a broad correlation margin, and neither have features too small to be resolved by the imaging system to be used nor large featureless areas. Applying speckles on the surface of the specimen using a sharpie marker can be a good technique for creating optimal speckle pattern. This type of technique is used on the surface of the specimens which are involved in measuring very high strains. To achieve this, dots on the surface were marked of the desired size. A black marker provides excellent contrast on a white base coat. An optimal speckle pattern is necessary for using DIC with ease for practical applications.

In order to assist a non-contact strain measurement system, an open source DIC software "Ncorr" was used as a tool for visualization of deformation history from initial unloaded stage to failure. This method is relatively easy to set up and deploys a cost-effective ordinary optical digital camera like a Digital Single-Lens Reflex Camera (DSLR) or smartphone camera, adapted

according to the situations (Suryanto *et al.* 2017).

The demand for cement has been continuously increasing because of the growing infra-structural activities of the country (Singh *et al.* 2015). It reveals that the necessity of cement in India is probably high and would touch 550 million tonnes by 2020 along with a shortage of 230 million tonnes (58%). Consumption of conventional concrete is greatly reduced by use of GPC leads to an eco-friendly and green construction as it is manufactured with environmental waste materials like fly ash, GGBS and rice husk ash etc. In the present work reinforced GPC beams are evaluated using DIC technique for determining the deflections and failure. The moment-curvature relationship is established for different grades conventionally and results are compared with those from DIC (Dutton *et al.* 2013, Swamy *et al*. 2018).

This study presents an innovative approach of using QR code as a speckle pattern in the field of DIC. The main objective is to compare the experimental results obtained from the readings of their deformations from the dial gauge and curvature meters with those obtained from DIC technique.

2. Experimental programme

The conventional program comprises of casting two beams each of three different concrete grades (total 24 beams), with both under-reinforced (UR) and over-reinforced (OR) sections. For each grade, two different types of speckle-pattern are used, one each for UR and OR sections. The random speckle pattern and QR code based random speckle pattern are used for both UR and OR sections with normal, medium and high strength concretes.

2.1 Materials used

Geopolymer concrete (GPC) is a new and alternative material for cement replacement. GGBS and fly ash were used as source materials in the present investigation. GGBS was collected from Toshali Cements Pvt Ltd, India. Fly ash was collected from a nearby National Thermal Power Plant, India. The specific gravity of GGBS and fly ash used were 2.90 and 2.17, respectively. The fineness of GGBS and fly ash were 426 m^2/kg and 380 m^2/kg. The chemical composition of GGBS and fly ash are shown in Table 1.

Table 1 Chemical composition of GGBS and Fly ash (% by mass)

Chemical Composition	GGBS	Fly ash
SiO_2	34	60.1
Al_2O_3	20	26.5
Fe_2O_3	0.8	4.2
SO_3	0.9	0.3
CaO	32.6	4.0
MgO	7.8	1.2
Na_2O	-	0.2
LOI	3.7	3.2

Table 2 Physical properties of Fine and Coarse Aggregates

Physical Properties	Fine Aggregate	Coarse Aggregate
Specific Gravity	2.64	2.81
Fineness Modulus	2.56	7.40
Bulk density (gm/cc)	1.46	1.40

Table 3 Mix Proportions obtained for GPC

Quantity	30 MPa	50 MPa	70 MPa
Fly ash + GGBS (kg/m^3)	360	450	520
Fly ash:GGBS	70:30	60:40	50:50
Fine Aggregate (kg/m^3)	776.39	760	718
Coarse Aggregate (kg/m^3)	1081	972	916
Alkaline Solution (kg/m^3)	203.5	248	286

Locally available river sand was used as fine aggregate, whereas, crushed granite was used as coarse aggregate. Fine aggregate corresponds to Zone II, while coarse aggregate with maximum size of aggregate 20 mm was used in this study. The physical properties of fine and coarse aggregates are shown in Table 2.

2.2 Mix proportions

Mix Proportions was done following the information from literature review (Rao *et al.* 2016, MLV and Kumar Rathish 2012, Patankar *et al.* 2013). The final mix proportions are presented in Table 3.

UR and OR beams of three different grades of concrete (30, 50 and 70 MPa) are cast and tested for deformations using dial gauges and curvature meters and DIC technique was employed to check its suitability of employing speckle patterns (Random and QR Code based random pattern).

3. Digital image correlation

3.1 General principle

DIC is based on comparing two images (reference image and deformed image) which are acquired at different states by a CCD (Charge Coupled Device) camera, before and after

deformations. After the acquisition, the images are digitized and two subsets are picked respectively from the reference and deformed images for correlation in form of a matrix (n×m). A fine search involving pixel by pixel is performed within the region of interest in the deformed image. The nearest location of the point of interest at the pixel level is selected based on the occurrence of the best-matched pattern which has the minimum value of mutual cross-correlation coefficient. Ncorr V1.2.2 uses an algorithm for correlation, which is programmed to detect the local displacement of a particular point by comparing the two image subsets and the result is in the form of pixel displacement. Pixel displacement is then converted to engineering units by using the camera to work effectively; the pixel blocks need to be random and unique with a range of contrast of 8-bit grey scale image intensity levels that vary from 0 to 255 shown in Fig. 2. It doesn't require any special lighting and in several cases, the natural surface of the structure or component has its own sufficient image texture for DIC to work without the necessity of special surface preparation.
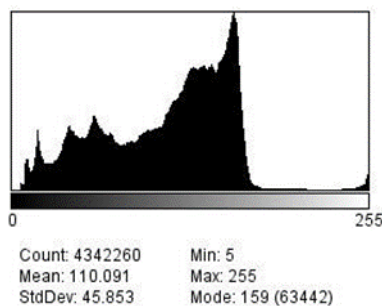

(a) Random speckle pattern   (b) QR code random speckle pattern
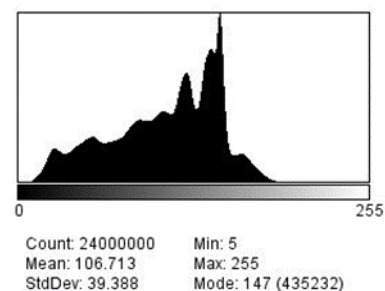
Fig. 1 Testing of RCC beams under four point loading

(a)   (b)

Fig. 2 Surface histogram of concrete beam (a) Random speckle pattern and (b) QR code based random speckle pattern showing grey scale intensity

(a) Using Random speckle pattern   (b) Using QR code random speckle pattern
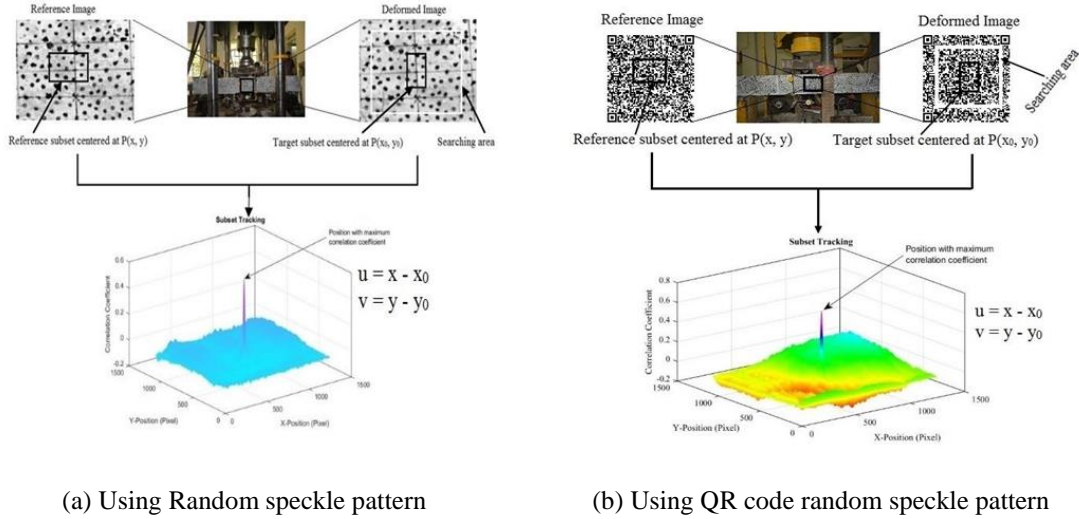
Fig. 3 Subset tracking procedure using DIC

Digital images are divided into a number of smaller regions which are termed subsets and these subsets undergo deformations when the image distortion takes place. The deformation location of the subset might not be at the integer location. That is why interpolation functions need to be used to get the gray intensity value at non-integer location.

The correlation function (C) is defined as the similarity between the deformed state and the undeformed state of the image subset. In general Pearson correlation coefficient lies between (-1 to +1) for optimal speckle patterns. To correlate the similarity index between the reference image subset and deformed image subset, a correlation analysis is done. In order to obtain the deformation subset, 2D DIC algorithm arrives at values of the extreme correlation cost function (Nguyen *et al.* 2017). This function can be written in the form

$$C = \frac{\int_{\Delta M} \left(F(x,y)\right) \left(G(x_0+U,y_0+V)\right) dA}{\left[\int_{\Delta M} [F(x,y)]^2 dA \int_{\Delta M} [G(x_0+U,y_0+V)]^2 dA\right]^{1/2}} \tag{1}$$

Where F and G are respectively references and deformed images having grayscale intensity functions at a specified location (x_o, y_o) and (x^1_o, y^1_o) a function of deformed location in Eq. (1).

Maximum correlation coefficient can be easily calculated using a simple Matlab® function. "normxcorr2" to find the correlation between two subsequent images (reference and deformed). It is clear that, the overall correlation is found to be higher in the case of QR code based random speckle pattern images from a three dimensional graph plotted between calculated correlation value and pixels, as shown in Fig. 3.

The physical size of 1 pixel might range between 1 nanometer to 1 centimeter approximately. DIC compares digital photographs of the test piece or component at different stages of deformation by identifying blocks of pixels. The system can also measure surface deformation as shown in Fig. 4 and full field 2D deformation vector fields and strain maps.
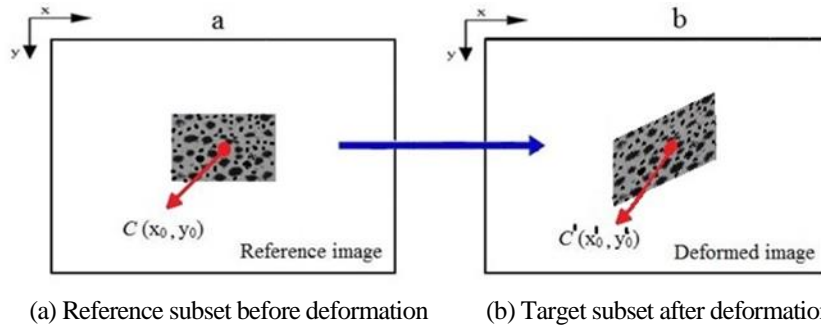
(a) Reference subset before deformation   (b) Target subset after deformation
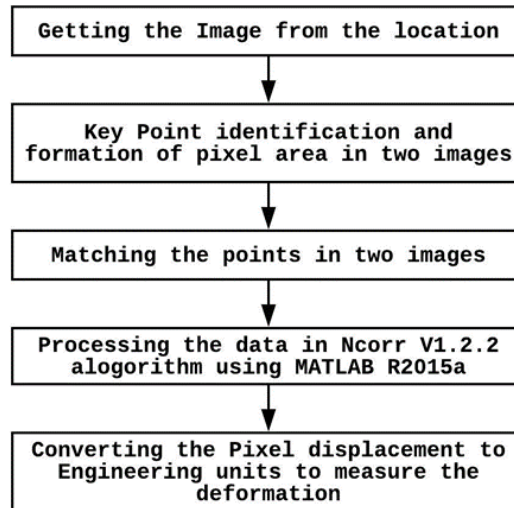
Fig. 4 Schematic representation of subsets

Fig. 5 Flowchart showing the image processing technique

3.2 Computation of strain measurement

In Cartesian coordinate system (x, y, z) the strain metrics can be calculated based on measured tangential displacement field (u, v, w) as shown in Eqs. (2)-(4). Strains are calculated from displacement data and the four displacement gradients are used to find the Lagrangian strains (Nguyen *et al.* 2017). Which are as follows

$$E_{xx} = 0.5 \left[2\frac{\partial u}{\partial x} + \left(\frac{\partial u}{\partial x}\right)^2 + \left(\frac{\partial v}{\partial x}\right)^2 \right] \tag{2}$$

$$E_{xy} = 0.5 \left[\frac{\partial u}{\partial y} + \frac{\partial v}{\partial x} + \frac{\partial u}{\partial x}\frac{\partial u}{\partial y} + \frac{\partial v}{\partial x}\frac{\partial v}{\partial y} \right] \tag{3}$$

$$E_{yy} = 0.5 \left[2 \frac{\partial v}{\partial y} + \left(\frac{\partial u}{\partial y} \right)^2 + \left(\frac{\partial v}{\partial y} \right)^2 \right] \qquad (4)$$

The flowchart shows in Fig. 5 briefly explains the procedure adopted for validation of DIC software along with the contact sensor devices.

This approach has been utilized successfully for large deformation measurements. Due to its simplicity, the DIC technique has been further extended to deformation and curvature studies. According to the technique, if the specimen attains the natural texture of random gray intensity value there is no necessity of specimen preparation for DIC.

3.3 DIC system setup

Two dimensional DIC technique presented in this study involves three consecutive steps, (1) Spraying speckle pattern on the specimen surface in order to obtain the random grey color intensity distribution; (2) Capturing the digital images of both undeformed and deformed specimen surfaces using low cost DSLR camera; (3) Post processing with Ncorr V1.2.2 DIC software for obtaining full-field displacement and strain. The minimum deflections/strains expected is measured in the order of 0.01 mm/micro strains. The size of the QR code is 150 mm by 150 mm, which was sprayed on flexural portion of the beam. The minimum radius of the subset considered in this study was 1.5 mm described circle with a step size of 1.5 mm up to 21 mm (as there was no significant difference in the results after 18 mm until 21 mm). The optimal radius of subset was found to be 13 mm based on the results obtained, which are in good agreement with conventional results.

4. Testing procedure

The experimental program is focused on comparison of the flexural behavior of reinforced GPC beams which is extracted using DIC technique for different speckle patterns. A comparison of conventionally measured moment and deformation/curvature obtained using combination of both QR Code based random speckle pattern and random speckle pattern is conducted. Low cost of-the-shelf equipment (Nikon D5200 DSLR camera with 24.1 MEGAPIXEL DX-format CMOS sensor) was used to capture the images while testing the RCC beams. After capturing the sequence of images, image processing was done by Ncorr, an open source DIC code using MATLAB® R2015a. The parameters varied in the investigation are normal (GPC 30 MPa), medium (GPC 50 MPa) and high strength (GPC 70 MPa) concretes as well as variation in the speckle patterns. Two different types of speckle patterns, random speckle pattern and QR Code based random speckle pattern are used. The cross section dimension of beams are 1800 mm × 150 mm × 200 mm. These beams are cast and tested for both UR and OR design category. Dial gauges (least count 0.01 mm) are used as conventional contact sensors and placed on the bottom surface of the beams to measure the deflections. The position of the Dial gauges is shown in Fig. 6. Curvature meters are used in compression zone as well as in tension zone and are 200 mm apart from the middle frame. The schematic drawing of the equipment, used for testing using random speckle pattern applied throughout the cross-section, is shown in Fig. 6.

The beams are quasi-statically tested using a UTM having a capacity of 1000 KN with a strain rate loading of 1.5 mm/min. With the application of loading and as the testing starts, images are captured at consecutive uniform intervals of loading using DSLR camera. The conventional results from the Dial gauges and curvature meters are then compared with DIC results.
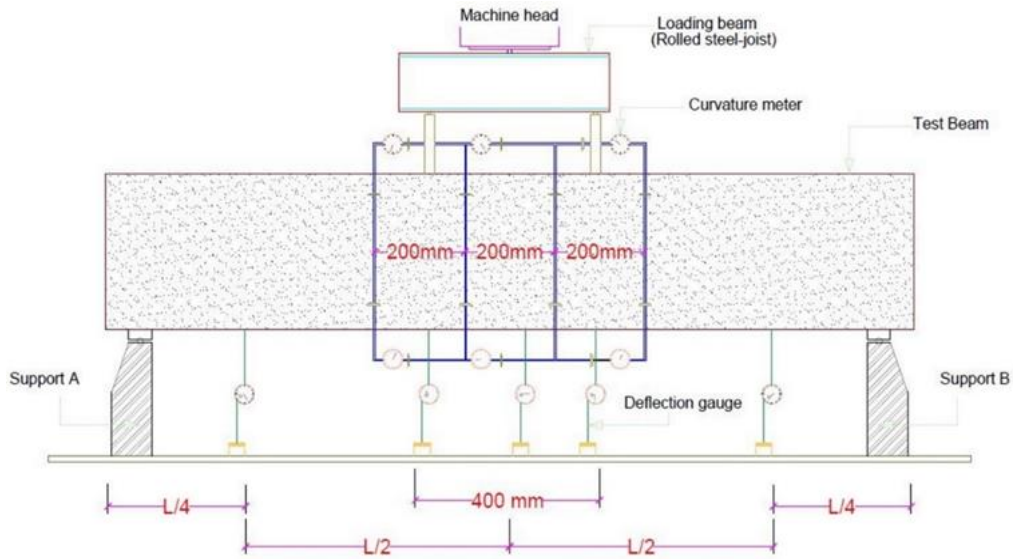
Fig. 6 Schematic diagram of Random Speckle Pattern test set-up

A QR code pattern stencil as shown in Fig. 7 is applied at critical locations of the beam surface for different beams (grades of concrete, OR and UR). In order to attain randomness of the pattern, QR codes are rotated and applied at critical locations. DIC results obtained using QR and random speckle are computed with deformation, curvature and strains obtained from conventional sensors. The schematic drawing of the equipment used for testing QR code random speckle pattern is shown in Fig. 8.
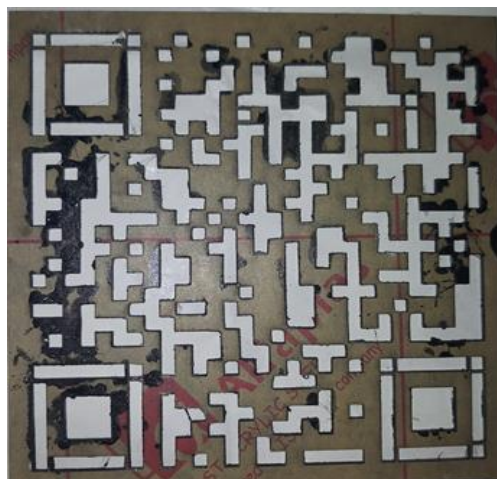
Fig. 7 Representative QR code pattern
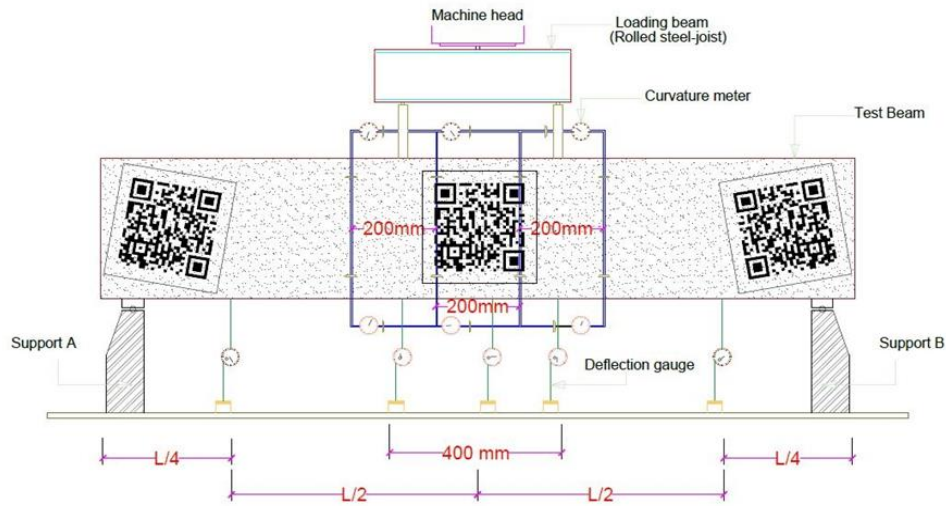
Fig. 8 Schematic diagram of QR Code with Random Speckle Pattern test set-up

5. Results and discussions

Beams of cross section size 1800 mm × 150 mm × 200 mm, are cast and tested to evaluate the load-deflection and moment-curvature relationships for both UR and OR beams. After completion of both the conventional and DIC analysis, flexural deflections corresponding to load obtained from the UTM are plotted. The averaged load vs flexural deflection of two beams, extracted from DIC using QR and random speckle patterns and compared with conventional measurements which is shown in Fig. 9.
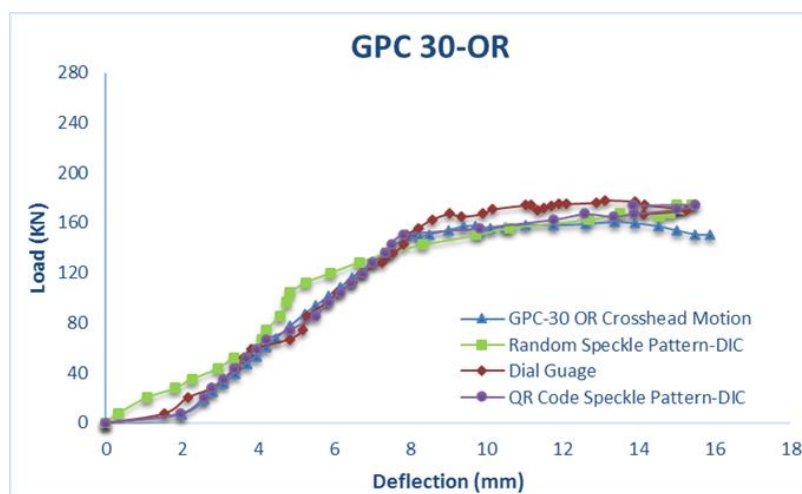

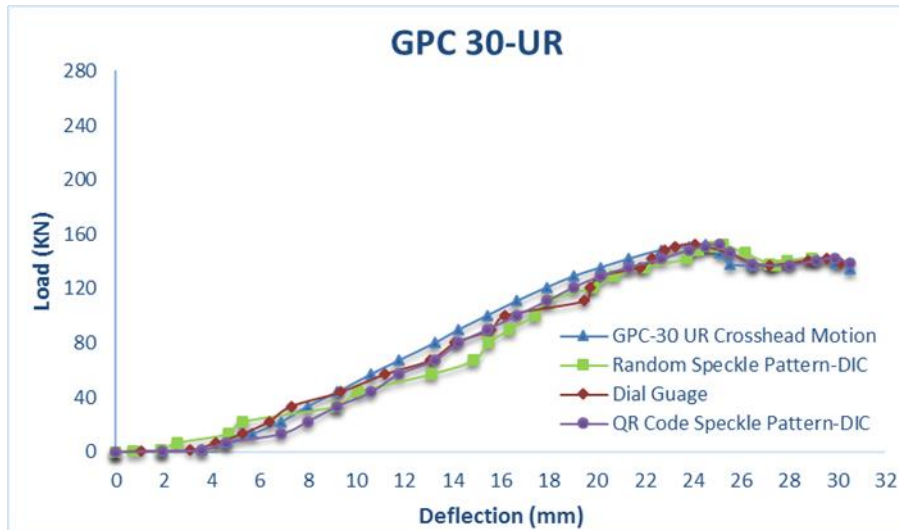Fig. 9 GPC 30 Over-Reinforced RCC concrete beam

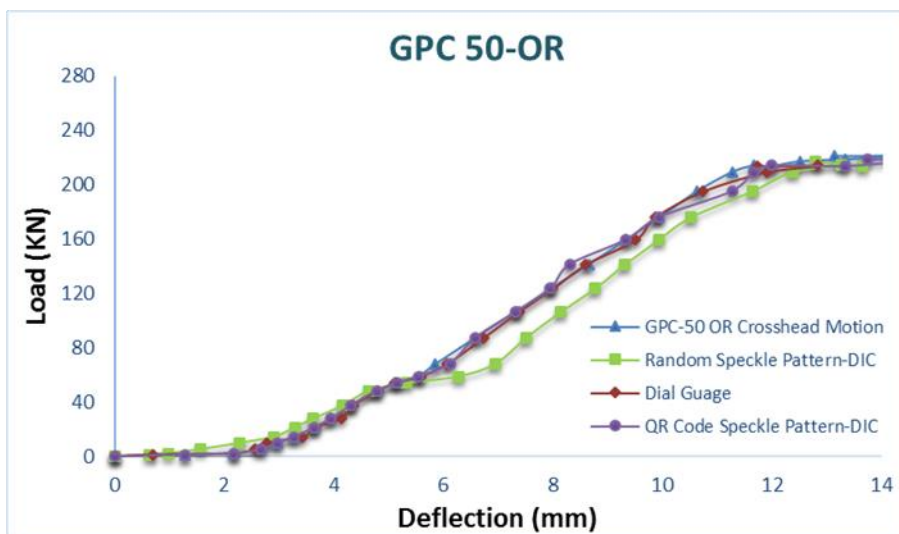Fig. 10 GPC 30 Under-Reinforced RCC concrete beam

Fig. 11 GPC 50 Over-Reinforced RCC concrete beam

Similarly, Figs. 9-14 shows a comparison of the conventional measurements and DIC with the crosshead movement of the conventional curve for GPC 30 (OR and UR), GPC 50 (OR and UR) and GPC 70 (OR and UR) specimens.
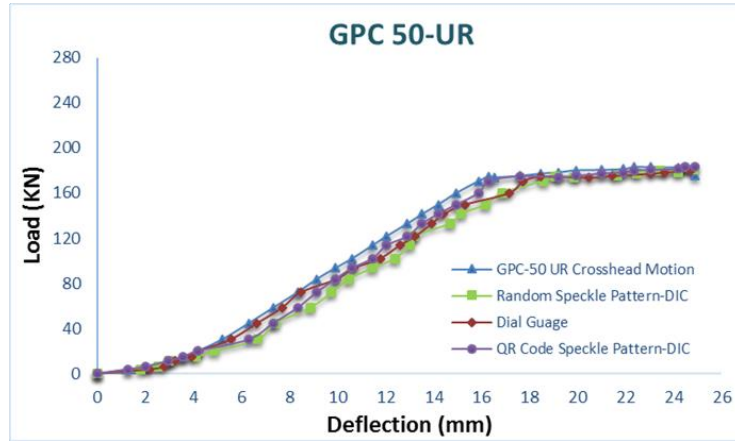
B. Murali Krishna et al.

Fig. 12 GPC 50 Under-Reinforced RCC concrete beam

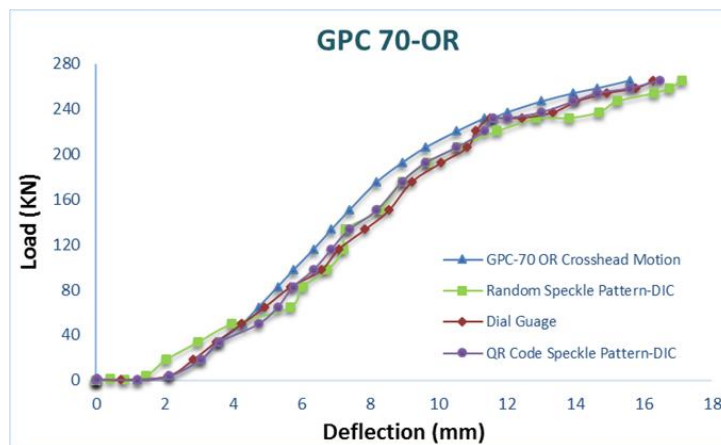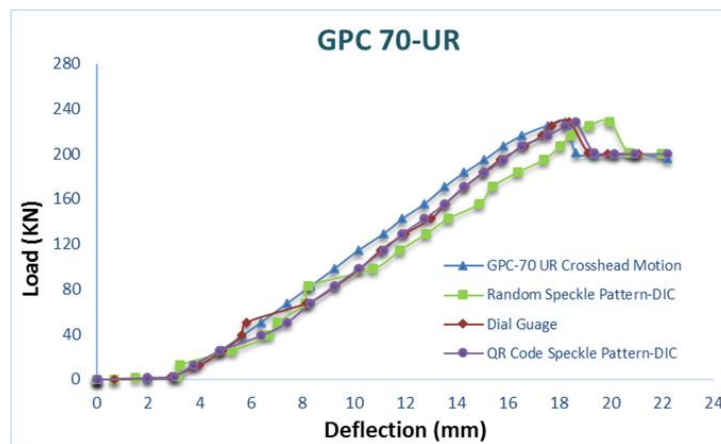

Fig. 13 GPC 70 Over-Reinforced RCC concrete beam

Fig. 14 GPC 70 Under-Reinforced RCC concrete beam

5.1 Experimental moment-curvature (M-κ) relationship

The curvature of the beams is measured by placing curvature meters in both the compression as well as in tension zones. Curvature meters having least count of 0.001 mm are fixed between two rectangular frames, one at the top and another at the bottom. Schematic view of the test setup is shown in Fig. 15. Based on radius of the top and bottom curvature meters, the average curvature is calculated. The deflections are measured using two load points, which is at the midpoint of the beam and at the points located midway between the supports and the midpoint, using dial gauges.

5.2 Comparison of the measured flexural behavior of concrete beams

A comparison of the moment-curvature values obtained from conventional (dial gauge, curvature meter and crosshead motion) measurements and DIC with different speckle patterns is shown in Figs. 16-18. Tables 4-6 shows the ultimate M-κ values of both UR and OR concrete GPC beams obtained from both conventional measurements and DIC technique using different speckle patterns.

Figs. 16-18 shows the M-κ relationship of both UR and OR beams with different speckle patterns for GPC beams. It is observed that the M-κ curves extracted using QR code random speckle pattern are closely match the curves obtained from conventional measurements.

As expected closely matching, the moment carrying capacity of OR beams is higher compared to UR beams. However, with the increase in grade of concrete the moment carrying capacity increases while the curvature of the beam at ultimate moment decreases.
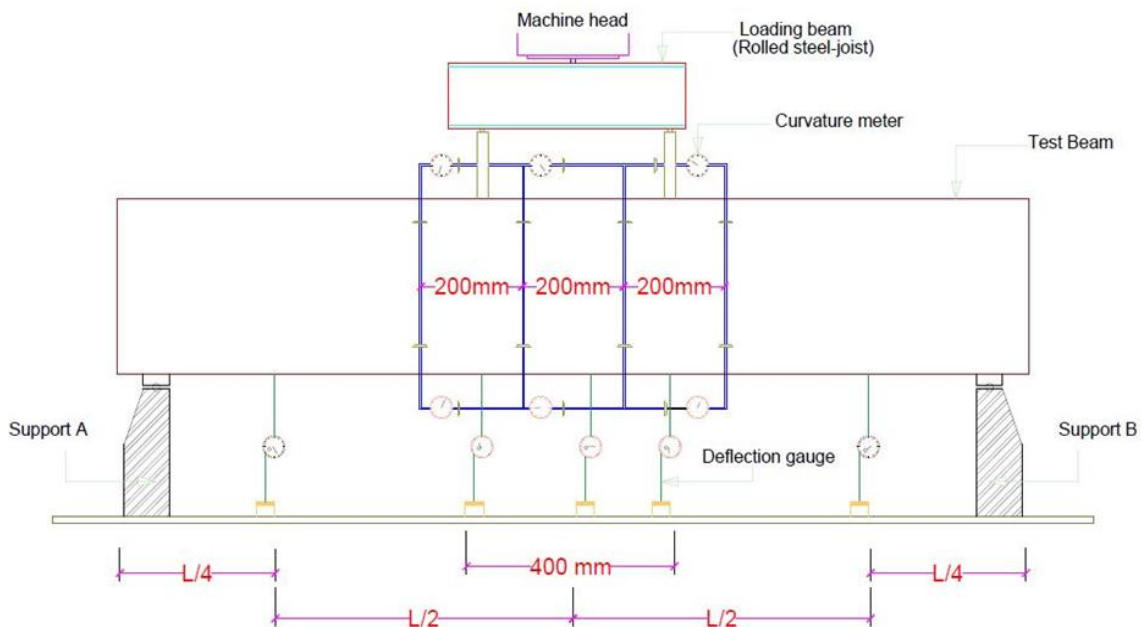

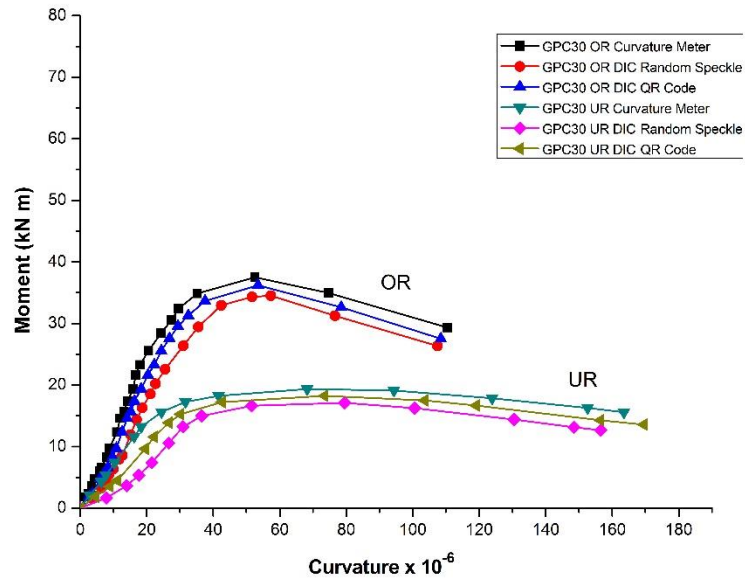Fig. 15 Schematic view of the test setup for Reinforced concrete beam
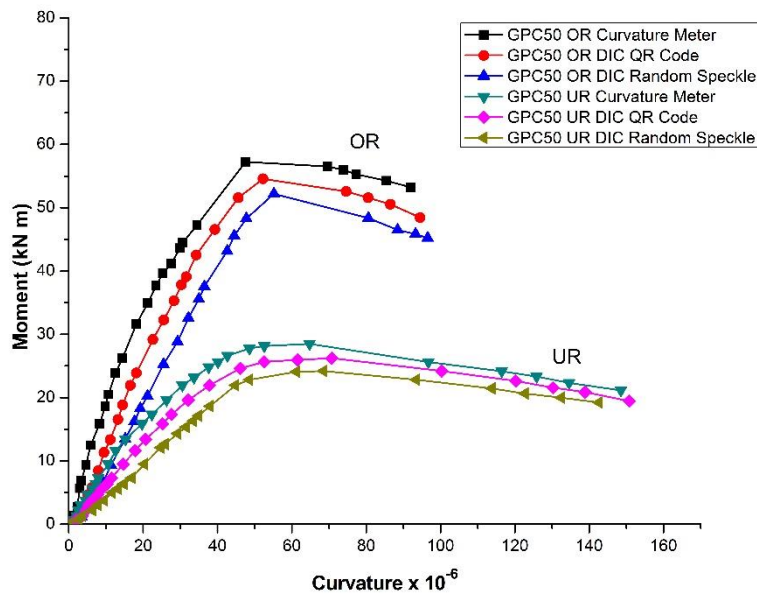
Fig. 16 M-κ curve for GPC 30 concrete grade

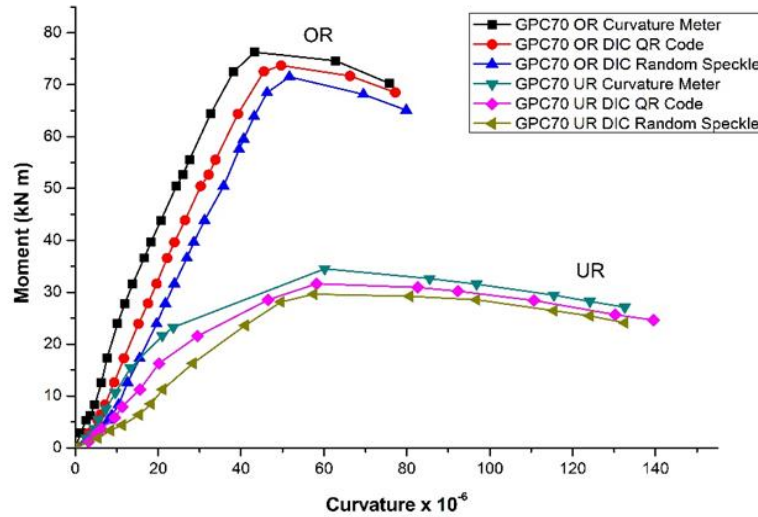Fig. 17 M-κ curve for GPC 50 concrete grade

Fig. 18 M-κ curve for GPC 70 concrete grade

5.3 Experimental M-κ at ultimate

Table 4 shows the experimental M-κ data for which ultimate values compared between normal (30 MPa), medium (50 MPa) and high strength (70 MPa)concretes for both UR and OR categories.

5.3.1 Digital image correlation M-κ at ultimate using random speckle pattern

Table 5 shows the DIC M-κ data at ultimate values where the beam is tested with random speckle throughout the cross-section of the beam. After testing the beam, results are extracted using Ncorr, a Matlab® based DIC software (Fig. 5). The results obtained from the software are compared with the conventionally obtained data.

Table 4 Ultimate moment and corresponding curvature, compressive strain and tensile strain obtained from conventional measurements

Grade	M (kN-m)	$\kappa \times 10^{-6}$	$\varepsilon_c \times 10^{-6}$	$\varepsilon_s \times 10^{-6}$
GPC 30 UR	19.35	68.23	2416	9865
GPC 30 OR	37.5	52.5	5054	4410
GPC 50 UR	28.5	64.77	2865	8794
GPC 50 OR	57.24	47.52	5375	3178
GPC 70 UR	34.54	60.21	3168	7670
GPC 70 OR	76.28	43.35	5841	1965

Table 5 Ultimate moment and corresponding curvature, compressive strain and tensile strain obtained using DIC (Random Speckle pattern)

Grade	M (kN-m)	$\kappa \times 10^{-6}$	$\varepsilon c \times 10^{-6}$	$\varepsilon s \times 10^{-6}$
GPC 30 UR	17.12	79.48	4333	9975
GPC 30 OR	34.51	57.33	6120	4200
GPC 50 UR	24.21	68.55	3760	8580
GPC 50 OR	52.21	55.18	5813	4120
GPC 70 UR	29.64	57.52	3121	7234
GPC 70 OR	71.55	51.65	7096	2201

5.3.2 Digital image correlation M-κ at ultimate using QR code as speckle pattern

Table 6 shows M-κ DIC data at ultimate values for which the beam was tested with QR Code based random speckle pattern.

Table 6 Ultimate moment and corresponding curvature, compressive strain and tensile strain obtained using DIC (QR Code)

Grade	M (kN-m)	$\kappa \times 10^{-6}$	$\varepsilon c \times 10^{-6}$	$\varepsilon s \times 10^{-6}$
GPC 30 UR	18.26	73.45	4007	9215
GPC 30 OR	36.21	53.46	5755	3869
GPC 50 UR	26.23	70.76	3922	8815
GPC 50 OR	54.58	52.26	5422	3986
GPC 70 UR	31.65	58.24	3125	7269
GPC 70 OR	73.71	49.68	6932	2012

Table 7 Comparison of ultimate moments and ultimate curvatures of beams obtained using Random and QR code random speckle patterns with that of conventional method of testing

Specimens Designation	Conventional		Random speckle pattern				QR code speckle pattern			
	M	κ	M	κ	M^1	κ^1	M	κ	M^1	κ^1
GPC 30 UR	19.35	68.23	17.12	79.48	11.52	16.49	18.26	73.45	5.63	7.65
GPC 30 OR	37.5	52.5	34.51	57.33	7.97	9.20	36.21	53.46	3.44	1.83
GPC 50 UR	28.5	64.77	24.21	68.55	15.05	5.84	26.23	70.76	7.96	9.25
GPC 50 OR	57.24	47.52	52.21	55.18	8.79	16.12	54.58	52.26	4.65	9.97
GPC 70 UR	34.54	60.21	29.64	57.52	14.19	4.47	31.65	58.24	8.37	3.27
GPC 70 OR	76.28	43.35	71.55	51.65	6.20	19.15	73.71	49.68	3.37	14.60

M^1 : % error in Moment (kN-m); κ^1 : % error in Curvature

Higher moment capacity is consistently observed when QR code based random speckle pattern is used in comparison with random speckle pattern. The maximum percentage error in ultimate moment is 15% in the case of random speckle pattern where as it reduces to 8% in case of combined QR code and random speckle patterns. The maximum percentage error in ultimate curvature is 19% in the case of random speckle pattern where as it reduces to 14% in case of combined QR code and random speckle patterns. The results obtained from the QR code based random speckle pattern are closer to the results obtained from conventional measurements.

6. Conclusions

Based on flexural response extracted using conventional measurements and DIC technique on GPC beams, the following conclusions are drawn:

- The M-κ relationships for GPC beams obtained from conventional dial gage and crosshead readings are compared with DIC results obtained using different speckle patterns. An innovative approach to use QR code as a speckle pattern in the field of DIC is proposed with comparative results.

- It is observed that M-κ values extracted using QR code based random speckle pattern compare well with conventionally obtained M-κ results. The ultimate moment carrying capacity of RCC (reinforced GPC) beams extracted from QR code based random speckle pattern is more consistent, with less scatter when compared with the ultimate values obtained from M-κ random speckle pattern.

- The more random the speckle pattern, closer are the DIC results are in comparison with conventional measurements.

- The QR code serves the dual purpose of embedding data in the structural component as well as functioning as random pattern for DIC which is helpful for non-contact sensor-based condition monitoring, as well as integration of component level data with BIM.

Acknowledgments

References

Antos, J., Nezerka, V. and Somr, M. (2017), "Assessment of 2d-dic stochastic patterns", *Acta Polytechnica CTU Proceedings*, **13**, 1-10.
Blaber, J., Adair, B. and Antoniou, A. (2015), "Ncorr: open-source 2D digital image correlation matlab software", *Exp. Mech.*, **55**(6), 1105-1122.
Bossuyt, S. (2013), Optimized patterns for digital image correlation. *In Imaging Methods for Novel Materials and Challenging Applications*, Springer, New York, NY. **3**, 239-248.

Carter, J.L., Uchic, M.D. and Mills, M.J. (2015), "Impact of speckle pattern parameters on DIC strain resolution calculated from in-situ SEM experiments", *In Fracture, Fatigue, Failure, and Damage Evolution*, **5**, 119-126.

Cofaru, C., Philips, W. and Van Paepegem, W. (2010), "Improved Newton–Raphson digital image correlation method for full-field displacement and strain calculation", *Appl. Opt.*, **49**(33), 6472-6484.

Dutton, M., Take, W.A. and Hoult, N.A. (2013), "Curvature monitoring of beams using digital image correlation", *J. Bridge Eng.*, **19**(3), 05013001.

Kozicki, J. and Tejchman, J. (2007), "Experimental investigations of strain localization in concrete using Digital Image Correlation (DIC) technique", *Arch. Hydro-Eng. Environ. Mech.*, **54**(1), 3-24.

Lecompte, D., Sol, H., Vantomme, J. and Habraken, A. (2006), "Analysis of speckle patterns for deformation measurements by digital image correlation", In SPECKLE06: Speckles, From Grains to Flowers, *International Society for Optics and Photonics*, **6341**, 63410E.

Long, X., Fu, S., Qi, Z., Yang, X. and Yu, Q. (2013), "Digital image correlation using stochastic parallel-gradient-descent algorithm", *Exp. Mech.*, **53**(4), 571-578.

Lu, H. and Cary, P.D. (2000), "Deformation measurements by digital image correlation: implementation of a second-order displacement gradient", *Exp. Mech.*, **40**(4), 393-400.

MLV, P. and Kumar Rathish, P. (2012), "Moment-curvature relationship of glass fiber reinforced self-compacting recycled aggregate concrete", *J. Environ. Res. Develop.*, **7**(2).

Mudassar, A.A. and Butt, S. (2016), "Improved digital image correlation method", *Opt. Laser. Eng.*, **87**, 156-167.

Nguyen, V.T., Kwon, S.J., Kwon, O.H. and Kim, Y.S. (2017), "Mechanical properties identification of sheet metals by 2D-digital image correlation method", *Procedia Eng.*, **184**, 381-389.

Pan, B., Qian, K., Xie, H. and Asundi, A. (2009), "Two-dimensional digital image correlation for in-plane displacement and strain measurement: a review", *Measur. Sci. Technol.*, **20**(6), 062001.

Patankar, S.V., Jamkar, S.S. and Ghugal, Y.M. (2013), "Effect of water-to-geopolymer binder ratio on the production of fly ash based geopolymer concrete", *Int. J. Adv. Technol. Civ. Eng.*, **2**(1), 79-83.

Rao, G.M., Rao, T.D., Seshu, R.D. and Venkatesh, A. (2016), "Mix proportioning of geopolymer concrete", *Cement Wapno Beton*, **21**(4), 274.

Salmanpour, A.H. and Mojsilovic, N. (2013), "Application of digital image correlation for strain measurements of large masonry walls", *Proceedings of the Conference APCOM & ISCM*, Singapore.

Singh, B., Ishwarya, G., Gupta, M. and Bhattacharyya, S.K. (2015), "Geopolymer concrete: A review of some recent developments", *Constr. Build. Mater.*, **85**, 78-90.

Su, C. and Anand, L. (2003), A new digital image correlation algorithm for whole-field displacement measurement.

Suryanto, B., Tambusay, A. and Suprobo, P. (2017), "Crack mapping on shear-critical reinforced concrete beams using an open source digital image correlation software", *Civil Eng. Dimension*, **19**(2), 93-98.

Sutton, M.A., Orteu, J.J. and Schreier, H. (2009), Image correlation for shape, motion and deformation measurements: basic concepts, theory and applications, *Springer Science & Business Media*.

Swamy Naga Ratna Giri, P., Rajesh Kumar, G., Sri Rama Chand, M. and Rathish Kumar, P. (2018). "Flexural behaviour of tie-confined self-curing self-compacting concrete", *Mag. Concrete Res.*, 1-11.

Vassoler, J.M. and Fancello, E.A. (2010), "Error analysis of the digital image correlation method", *Mecánica Computacional*, **29**(61), 6149-6161.

Yuan, Y., Huang, J., Fang, J., Yuan, F. and Xiong, C. (2015), "A self-adaptive sampling digital image correlation algorithm for accurate displacement measurement", *Opt, Laser. Eng.*, **65**, 57-63.

JK